Detection and characterization of mosaicism in autosomal dominant polycystic kidney disease

see commentary on page 261

Katharina Hopp[1,2], Emilie Cornec-Le Gall[2,3,4], Sarah R. Senum[2], Iris B.A.W. te Paske[2], Sonam Raj[2], Sravanthi Lavu[2], Saurabh Baheti[5], Marie E. Edwards[2], Charles D. Madsen[2], Christina M. Heyer[2], Albert C.M. Ong[6], Kyongtae T. Bae[7], Richard Fatica[8], Theodore I. Steinman[9], Arlene B. Chapman[10,11], Berenice Gitomer[1], Ronald D. Perrone[12], Frederic F. Rahbari-Oskoui[11], Vicente E. Torres[2], the HALT Progression of Polycystic Kidney Disease Group, the ADPKD Modifier Study, and Peter C. Harris[2,13]

[1]Division of Renal Diseases and Hypertension, University of Colorado Denver Anschutz Medical Campus, Aurora, Colorado, USA; [2]Division of Nephrology and Hypertension, Mayo Clinic, Rochester, Minnesota, USA; [3]Department of Nephrology, Centre Hospitalier Universitaire de Brest, Université de Brest, Brest, France; [4]National Institute of Health and Medical Sciences, INSERM U1078, Brest, France; [5]Division of Biomedical Statistics and Informatics, Mayo Clinic, Rochester, Minnesota, USA; [6]Kidney Genetics Group, Academic Nephrology Unit, University of Sheffield, Sheffield, UK; [7]Department of Radiology, University of Pittsburgh School of Medicine, Pittsburgh, Pennsylvania, USA; [8]Department of Nephrology and Hypertension, Cleveland Clinic, Cleveland, Ohio, USA; [9]Renal Division, Beth Israel Deaconess Medical Center, Boston, Massachusetts, USA; [10]Division of Nephrology, University of Chicago School of Medicine, Chicago, Illinois, USA; [11]Department of Internal Medicine, Emory University School of Medicine, Atlanta, Georgia, USA; [12]Division of Nephrology, Tufts University Medical Center, Boston, Massachusetts, USA; and [13]Department of Biochemistry and Molecular Biology, Mayo Clinic, Rochester, Minnesota, USA

Autosomal dominant polycystic kidney disease (ADPKD) is an inherited, progressive nephropathy accounting for 4-10% of end stage renal disease worldwide. *PKD1* and *PKD2* are the most common disease loci, but even accounting for other genetic causes, about 7% of families remain unresolved. Typically, these unsolved cases have relatively mild kidney disease and often have a negative family history. Mosaicism, due to *de novo* mutation in the early embryo, has rarely been identified by conventional genetic analysis of ADPKD families. Here we screened for mosaicism by employing two next generation sequencing screens, specific analysis of *PKD1* and *PKD2* employing long-range polymerase chain reaction, or targeted capture of cystogenes. We characterized mosaicism in 20 ADPKD families; the pathogenic variant was transmitted to the next generation in five families and sporadic in 15. The mosaic pathogenic variant was newly discovered by next generation sequencing in 13 families, and these methods precisely quantified the level of mosaicism in all. All of the mosaic cases had *PKD1* mutations, 14 were deletions or insertions, and 16 occurred in females. Analysis of kidney size and function showed the mosaic cases had milder disease than a control *PKD1* population, but only a few had clearly asymmetric disease. Thus, in a typical ADPKD population, readily detectable mosaicism by next generation sequencing accounts for about 1% of cases, and about 10% of genetically unresolved cases with an uncertain family history. Hence, identification of mosaicism is important to fully characterize ADPKD populations and provides informed prognostic information.

Correspondence: *Peter C. Harris, Division of Nephrology and Hypertension, Mayo Clinic, Stabile 7, 200 First Street SW, Rochester, Minnesota 55905, USA. E-mail: harris.peter@mayo.edu*

Received 4 June 2019; revised 5 August 2019; accepted 29 August 2019; published online 9 October 2019

Kidney International (2020) **97,** 370–382; https://doi.org/10.1016/j.kint.2019.08.038

KEYWORDS: ADPKD; diagnostics; genotype/phenotype correlations; mosaicism; mutations; PKD1; prognostics

Copyright © 2019, International Society of Nephrology. Published by Elsevier Inc. All rights reserved.

Tuberous sclerosis is an example of a dominant disease in which *de novo* mutations are common, accounting for 60%–70% of cases.[1] These new mutations usually happen in germ cells but can occur postzygotically, resulting in mosaicism in which the subject is composed of cells with and without the mutation. Mosaic pathogenic variants can be difficult to detect by Sanger sequencing (SS), and when targeted-capture next-generation sequencing (tNGS) was applied to the 10%–15% of tuberous sclerosis patents with no (Sanger) mutation identified (NMI), 49% were found to be mosaics.[2] Hence, mosaicism is a diagnostic challenge, but its identification is important to fully characterize a population for family planning purposes, and to determine likely disease severity within a family.

Population studies indicate that 10%–20% of ADPKD families can be traced to a *de novo* mutation within living generations.[3,4] ADPKD is a late-onset, systemic, inherited disorder with a worldwide prevalence[5] of ~1 in 1000. It is characterized by the development and growth of kidney cysts, resulting in end-stage renal disease in ~50% of individuals by age 60 years.[6] The major ADPKD genes are *PKD1* (~78% of pedigrees) and *PKD2* (~15%); PKD1 is associated with more-severe disease, and *PKD1* truncating (*PKD1*^{T}) alleles are

more severe than nontruncating alleles (*PKD1*^{NT}).[7–9] A small proportion of NMI cases have mutations to other genes, e.g., *GANAB*, *DNAJB11*, or *HNF1B*, but ~7% remain unresolved.[10–13] Mutation screening of *PKD1* is complicated by the presence of 6 pseudogenes, traditionally requiring a long-range polymerase chain reaction (LR-PCR) approach for SS.[14] More recently, LR-NGS and specifically designed tNGS approaches have been shown to successfully screen this locus.[15–18]

Mosaicism is a possible explanation for NMI cases, as they often have a negative/indeterminate family history, typically milder disease, and sometimes an asymmetric/unilateral renal disease presentation; 5 mosaic ADPKD families have been described.[4,9,19] One with gonadal and somatic mosaicism (mixed) illustrated the complexity of identifying a potential living related donor by linkage analysis alone.[20] In a second, an affected father with 2 ADPKD daughters had the familial large deletion in just ~15% of cells.[21] Other examples showed milder than expected disease for a *PKD1*^{T} pathogenic variant in a mosaic mother[22]; LR-NGS analysis detected low-level mosaicism (3%–10%) in different cell types[23]; and quantitative PCR and cloning detected mosaicism in a patient with asymmetric disease.[4] Importantly, all described cases were identified because an offspring had fully penetrant disease.

Here, we employed 2 NGS approaches to detect and characterize mosaicism in 20 ADPKD pedigrees.

RESULTS

Next-generation sequencing analysis to detect mosaicism

To detect mosaicism, 2 NGS methods were employed—a modified LR-NGS screen[15] of just *PKD1* and *PKD2* and a tNGS panel of 65 or 137 cystogenes (Figure 1; Supplementary Table S1),[12] with DNA isolated from blood cells, mimicking a clinical diagnostic setting. The LR-NGS screen included 106 ADPKD families with a known/suspected negative family history and NMI from SS of *PKD1* and *PKD2*. Four suspected mosaics detected by family/conventional analysis were controls (Figure 1). The tNGS screening included 2 parts—408 SS *PKD1*/*PKD2* NMI ADPKD-like families,[12] and 445 unscreened ADPKD-like families (Figure 1). Previous analysis showed good coverage of the duplicated *PKD1* gene using this

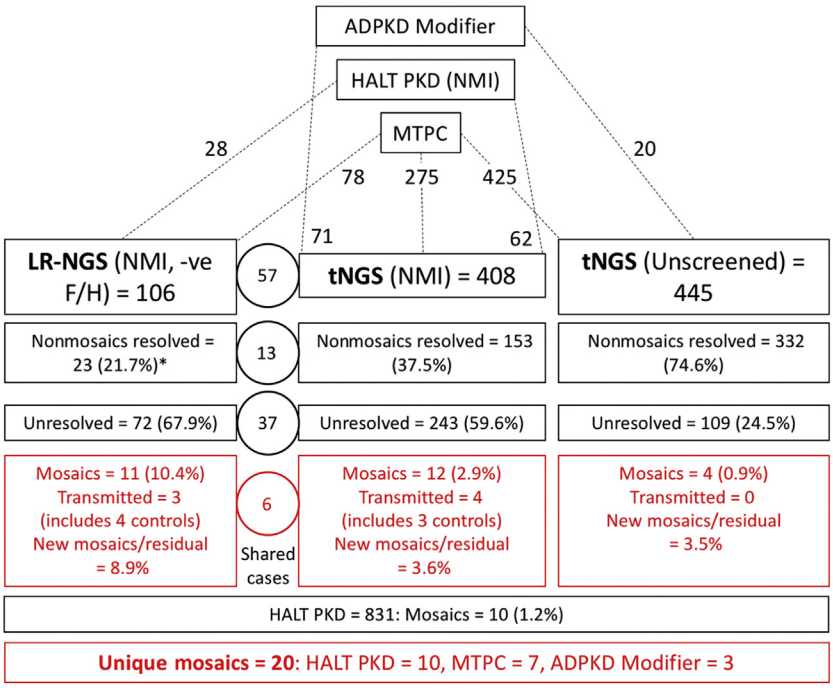

Figure 1 | Diagram showing the study design and detection rates for the different groups involved in the screen for mosaicism. Autosomal dominant polycystic kidney disease (ADPKD) patients were included in the study from those collected for mutation screening at the Mayo Translational PKD Center (MTPC), ADPKD Modifier patients, and *PKD1* and *PKD2* Sanger sequencing (SS), no (Sanger) mutation identified (NMI) HALT PKD patients. The analysis for mosaic cases was performed in 3 screens: long-range next-generation sequencing (LR-NGS) of *PKD1* and *PKD2* SS NMI ADPKD patients with a proven or suspected negative family history (–ve F/H); a targeted-capture (t)NGS screen of *PKD1* and *PKD2* SS NMI ADPKD patients; and a tNGS screen of previously unscreened patients. The number of total families included in each screen, and their origin, is indicated at the top portion of the figure. The detection rate breakdown of each screen is indicated in boxes and includes number of families resolved with typical heterozygous variants (nonmosaics resolved), number of families remaining unresolved, and the number of families with detected mosaic variants. The numbers in the circles represent families shared among the LR-NGS and tNGS approaches. The number of newly detected mosaics as a proportion of the unresolved plus mosaics (new mosaics/residual) is also calculated. Approximately 1% of families (HALT PKD [1.2%] and tNGS [unscreened, 0.9%]) were mosaics. In addition, newly resolved mosaics represented 8.9% of the unresolved plus mosaic families from the LR-NGS screen (–ve F/H and SS *PKD1/PKD2* NMI) and 3.6% from the tNGS (SS *PKD1/PKD2* NMI) screen. The number of unresolved families from the tNGS (unscreened) analysis is greater than expected from a typical ADPKD population, which is likely because of the large number of very mild and atypical patients screened from the MTPC population. *For the nonmosaic patients resolved from the LR-NGS screen, results from other genes detected by tNGS are also included.

tNGS approach.[12] Both screening methods have the advantage over whole-exome sequencing of having a high average sequence read depth (LR-NGS *PKD1* = 7317, *PKD2* = 10,988; 65-Gene-tNGS *PKD1* = 839; *PKD2* = 475; 137-Gene-tNGS *PKD1* = 619; *PKD2* = 779; Supplementary Table S2), allowing detection of pathogenic variants found in just a small percentage of reads.

Two families illustrated the need for caution in defining mosaic cases and the value of employing NGS plus Sanger methodologies. In pedigree M796, SS of individual II-2 suggested a missense pathogenic variant at a low level, but subsequent tNGS analysis showed that 581 of 1130 reads (51%) had the pathogenic variant (Supplementary Figure S1A–C). Follow-up SS consistently showed a low-level signal of the pathogenic variant (Supplementary Figure S1B). These SS findings are likely explained by allele dropout due to a polymorphism under the LR or exon-specific PCR primer. Family P1317 showed the opposite scenario, in which tNGS identified a 26–base pair (bp) duplication in just 7.9% of reads in II-1 (Supplementary Figure S1D and E). However, SS showed the duplication to be equally represented (Supplementary Figure S1F), and subsequently the patient was found to have a positive family history, highlighting the fact that with use of tNGS, larger duplications may be captured inefficiently.

Definitions and details of the detected mosaic cases

To be certain that the described cases are genuine mosaics, we required the pathogenic variant to be consistently detected at a reduced level by NGS, and SS or allele-specific PCR (AS-PCR). To avoid identifying cases as mosaics that had apparent small reductions in read representation, as these can be false mosaics, or false positives for being resolved, the mutant allele needed to be present in 2%–25% of reads (4%–50% of the expected level of the pathogenic allele); 2 exceptions (Pedigrees 390010 and 790057) are explained later. Table 1 and Supplementary Table S3 describe and evaluate the detected mosaic pathogenic variants to *PKD1* and provide clinical information on the 20 resolved families. All families have a negative or equivocal family history, with details and diagnostic information summarized in Table 2.

Families with a transmitted *PKD1* mosaic variant (mixed)

In 5 families, the mosaicism was somatic, but the pathogenic variant was also germinal, since the mutation was transmitted to the next generation. Mosaicism was suspected from SS of Family 590013 since the frameshifting change detected in the son (III-1) was only apparent at a low level in the affected mother (II-2; Figure 2a and b). tNGS analysis confirmed the mutant allele in just 157 of 906 reads (17.3%), compared with 702 of 1415 (49.6%) in III-1 (Figure 2c). Asymmetric disease was seen in II-2, with a few large cysts in the left kidney, in contrast to multiple small cysts detected in III-1 (Figure 2d and e). II-2 had normal renal function at age 56 years.

In Family 690020, a *PKD1*^{T} pathogenic variant was readily detected by SS in III-1, but it was found in the mother (II-2) only after focused analysis (Figure 2f and g). LR-NGS identified the change in II-2 in 589 of 6476 reads (9.1%). II-2's ultrasound imaging showed moderately enlarged kidneys at age 61 years, whereas III-1 had significantly enlarged kidneys (Mayo Imaging Class MIC-1C[8]; Supplementary Figure S2A); II-2 had just mild renal impairment at age 67 years.

Individual 870348 II-2 was initially screened by tNGS and found to have a deletion in 515 of 6247 reads (8.2%; Figure 2h). The deletion was confirmed at a low level by SS and AS-PCR (Figure 2i; Supplementary Figure S2B). II-2 had multiple bilateral cysts (MIC-1B), with normal renal function at age 47 years (Figure 2j). One son, III-1, was diagnosed at age 26 years.

Initial SS of 590046 II-4 did not identify a likely mutation; however, SS of the son (III-2) detected a single codon deletion (Supplementary Table S3). LR-NGS of II-4 showed that 899 of 12858 reads (7.0%) had the deletion, which was confirmed by close inspection of the Sanger sequence (Figure 2k and l). II-4 had an atypical radiological presentation (MIC-2A), with one large kidney and liver cyst and normal renal function at age 56 years (Figure 2m). Two sons were affected, and mild cystic disease (MIC-1B) was characterized in III-2 at age 19 years (Figure 2n).

SS of 390010 III-1 identified a large inframe deletion (Supplementary Table S3), but it was not detected in his affected mother (II-2; Figure 2o). LR-NGS also did not readily detect the variant in II-2, but careful analysis showed that 6 of 4246 reads (0.1%) contained the deletion. SS of AS-PCR showed the deleted sequence in III-1, and a mixture of the normal and deleted sequence in II-2, reflecting an enrichment of the rare deleted sequence (Figure 2p). Imaging of II-2 showed very mild cystic disease (MIC-1A) at age 48 years and normal renal function at age 52 years, whereas the disease in III-1 was more typical for an *PKD1* fully penetrant pathogenic variant (MIC-1D; Figure 2q and r).

Families with a mosaic variant in a single individual (somatic)

Fifteen families had a somatic mosaic *PKD1* pathogenic variant that was not shown to be transmitted. 790057 II-2 was suspected of having a whole-exon deletion, determined from multiplex ligation-dependent probe amplification (MLPA), but the level of signal suggested mosaicism (Figure 3a and b). Reanalysis by LR-NGS confirmed the deletion, and SS of a breakpoint fragment defined the deletion (Figure 3c; Supplementary Figure S2C). Analysis of read depth within (4731) and flanking the deletion (7810) indicated that 37.7% reads had the deletion—a margin, along with the MLPA data, consistent with mosaicism. The disease of II-2 was moderately severe (MIC-1C; Figure 3d), but with normal renal function at age 31 years.

In 590039 II-4, MLPA detected an apparently mosaic multi-exon deletion (Figure 3e and f). The deletion was

Table 1 | Clinical presentation and genetic details of PKD1 families with mosaicism

			% Reads positive					Image analysis								
								Kidney							Liver	
										Vol (ht)						
Pedigree	Pathogenic variant	Subject	LR-NGS	tNGS	Sex	eGFR age (yr)	HTN age (yr)	Age (yr)	Cystic description	RK	LK	TKV	MIC	Fig	Cystic description	Vol (ht)
Variant transmitted																
590013	c.935_937delinsA	II-2	NS	17.3	F	63/56	43	52	Multiple bilateral, large LK	249	639	888	1C	2d	Some small	1013
	p.(Ala312fs)	III-1	Offspring		M	67/29	18	25	Multiple bilateral	326	396	722	1E	2e	Few very small	828
690020	c.12440_12443dup	II-2	9.1	NS	F	57/67	61	61	Many large bilateral (ultrasound)	14.2[a]	16.6[a]	NA	ND		5.3-cm cyst	NA
	p.(Phe4149fs)	III-1	Offspring		F	109/43	41	42	Multiple bilateral	402	424	826	1C	S2A	Few small	947
870348	c.2548_2557del	II-2	NS	8.2	M	87/47	36	47	Multiple bilateral	244	351	595	1B	2j	Few small	696
	p.(Asp850fs)	III-1	Offspring		M	Diagnosed at 26 yr but no further information available										
590046	c.8970_8972del	II-4	7.0	NS	F	91/56	Y/22	53	Multiple tiny, 1 large LK	223	325	548	2A	2m	One large cyst	1529
	p.(Tyr2991del)	III-2	Offspring		M	127/22	NA	19	Few bilateral	120	114	234	1B	2n	No cysts	951
		III-4	Offspring		M	NA	NA	11	Multiple bilateral (ultrasound)			NA	ND		NA	
390010	c.11654_11683del	II-2	0.1	ND	F	74/52	N/51	48	Few, 1 large RK and LK	113	144	257	1A	2q	Few tiny	777
	p.(Val3885_Ser3894del)	III-1	Offspring		M	82/38	20	35	Multiple bilateral	373	436	809	1D	2r	Multiple small	1054
Single affected individual																
790057	c.1386-34_1606+26del282bp, p.(Ser463fs)	II-2	NI	37.7	F	82/37	Y/29	31	Multiple bilateral	303	348	651	1C	3d	Few large	1382
590039	c.215+8043_1850-141del11.7kb, p.(Leu72fs)	II-4	NI	22.7, 25.5[a]	F	ES/55 28/53	Y/39	49	Multiple large bilateral	785	1073	1858	1D	3h	Severe PLD	4228[b]
M484	c.10922dupC, p.(Arg3642fs)	II-8	20.6	20.1	F	88/47	Y/44	46	Many large bilateral	400	573	973	1C	3k	Severe PLD	3334
M375	c.11379delG, p.(Thr3794fs)	II-3	19.1	NS	F	113/34	N/34	37	Multiple small	97	136	233	1A	3n	Few small	908
290001	c.4520G>A, p.(Trp1507*)	II-1	17.5	20.6	F	41/66	Y/42	42	Multiple bilateral (ultrasound)			NA	ND		NA	
870005	c.844_845dupGG, p.(Pro283fs)	II-2	NS	14.8	F	72/54	Y/43	49	Many large bilateral	400	431	831	1C	4c	Moderate PLD	NA
M646	c.8426C>T, p.(Pro2809Leu)	II-3	NS	13.4	M	44/60	Y/<54	54	Bilateral, several large LK	206	282	487	1B	4f	None	1191
870452	c.11157-2A>G, p.(Arg3719?)	II-2	NS	13.4	F	77/57	Y/45	52	Multiple bilateral	527	735	1262	1C		~70 small	NA
M1312	c.5352_5353insTG, p.(Asn1785*)	II-2	NS	12.2	F	125/35	N/36	36	Multiple, 1 large RK	280	256	536	1C	4k	Few tiny	536
290034	c.3685delG, p.(Val1229fs)	II-3	12.3	12.0	M	34/68	Y/52	67	Bilateral renal enlargement	1506	1179	2685	1C		NA	NA
M1327	c.10373_10386del14, p.(Pro3458fs)	II-2	NS	9.0	M	78/48	Y/40	46	Multiple cysts, few large	186	198	384	1B	5c	Few small	876
M855	c.74_75delGCinsT, p.(Gly25fs)	II-4	8.2	NS	F	76/47	N/47	39	Multiple small RK, few LK	230	103	333	1B	5f	Multiple small	847
290084	c.1722G>T[c], p.(Glu574?)	II-7	6.0	7.3	F	74/53	Y/44	50	Many large bilateral	439	359	798	1C	5i	Severe PLD	4173
M174	c.12682C>T, p.(Arg4228*)	II-1	7.1	3.5	F	ES/83 16/83	Y/64	82	Few large bilateral	512	742	1254	1B	5l	Multiple small	649
290114	c.9185_9201+7del24, p.(Val3062fs)	II-1	4.1	1.3	F	70/40	Y/34	38	Multiple small, 3 large LK	278	164	442	1B	5o	Few small	1299

eGFR, estimated glomerular filtration rate; ES, end-stage renal disease; F, female; Fig, figure within this article; HTN, hypertension; LK, left kidney; LR-NGS, long-range next-generation sequencing; M, male; MIC, Mayo Imaging Class; N, no; NA, not available; ND, not detected; NI, not informative; NS, not screened; PLD, polycystic liver disease; RK, right kidney; TKV, total kidney volume; tNGS, targeted-capture next-generation sequencing; Vol (ht), height-adjusted kidney or liver volume; Y, yes; yr, years.

[a]Kidney length.

[b]Value before liver resection.

[c]Predicted to disrupt splicing.

Table 2 | Diagnostic and family history details of PKD1 patients with mosaicism

Pedigree	Subject	Proband diagnosis: Age (yr)	Why	Initial molecular	Confirmed molecular	Family history: Father	Mother	Siblings	Children	Comments
Variant transmitted										
590013	II-2	28	Pregnancy, US	FH/ Sanger	tNGS	80 yr[a], PC, 79 yr BRC	87 yr, no PKD Dx	2, no PKD Dx	1 +ve, HALT A, III-1	Father had some cysts
690020	II-2	61	severe HTN, US	FH/ Sanger	LR-NGS	>90 yr, no PKD Dx	~40 yr, LTFU, no PKD Dx	2, no PKD Dx	1 +ve, HALT A, III-1 2 GD, +ve US 19 yr and <19 yr	Father reported kidney and AAA problems
870348	II-2	44	HTN, enlarged kidneys	tNGS	Sanger/ ASPCR	No PKD Dx	No PKD Dx	2, no PKD Dx	1 +ve 26 yr, 1 untested	
590046	II-4	46	NA	FH/ Sanger	LR-NGS	-ve US 78 yr	-ve US 76 yr	2 -ve US, 50, 37 yr, 2[a] other causes	2 +ve 16 yr, 11 yr, 1 -ve US 10 yr, 1 RF untested	Brother[a] encephalopathy, sister MRKH, III-4, PH
390010	II-2	39	Pain, US	FH/LR-NGS	AS-PCR	76 yr[a] cardiac, no PKD Dx	80 yr[a], no PKD Dx	2, no PKD Dx, 1[a] accidental	1 +ve, HALT A, 1, BRC, LTFU	
Single affected individual										
790057	II-2	30	HTN, MR	MLPA	tNGS	No PKD Dx	No PKD Dx, stones	3, no PKD Dx	2, untested	
590039	II-4	32	Pain, imaging	MLPA	tNGS/CNV	68 yr[a], no PKD Dx	74 yr, no PKD Dx	4, no PKD Dx, 1 sister liver cysts	1, no PKD Dx	Distant relatives with PKD?
M484	II-8	37	Fullness, possible mass, imaging	2× NGS	Sanger	50 yr[a], alcoholic, no PKD Dx	No PKD Dx	6, no PKD Dx	2, no PKD Dx	
M375	II-3	26	CT, pain	Sanger	LR-NGS	[a]MI, no PKD Dx	2 liver cysts	3, no PKD Dx	None	
290001	II-1	42	US	2× NGS	Sanger	No PKD Dx	No PKD Dx	None	2 -ve US, 20 yr, 14 yr, 1 untested	
870005	II-2	43	Pain, imaging	tNGS	Sanger	[a]Melanoma, no PKD Dx	No PKD Dx	1, no PKD Dx	3, untested	
M646	II-3	53	HTN, US	tNGS	Sanger	No PKD Dx	No PKD Dx	4, no PKD Dx	1, no PKD Dx	
870452	II-2	45	HTN, flank pain, imaging	tNGS	Sanger	No PKD Dx, 76 yr	No PKD Dx, 75 yr	1, no PKD Dx, 57 yr	1 -ve US, 2 untested	Grandfather end-stage renal disease 75 yr
M1312	II-2	25	Pregnancy US	tNGS	AS-PCR	-ve US	-ve US	1, -ve US	4 untested	6-mm kidney stone
290034	II-3	56	Hematuria, imaging	2× NGS	Sanger	77 yr[a], no PKD Dx	No PKD Dx	2, no PKD Dx	1 no PKD, 1 untested	
M1327	II-2	46	Cyst hemorrhage	tNGS	Sanger	-ve US, ~70 yr, MND	-ve US, 70 yr, MND	2, no PKD Dx	3 untested	
M855	II-4	38	Pain, US	Sanger	LR-NGS	-ve US, 72 yr	-ve US, 68 yr	3, no PKD Dx	3 no PKD Dx	
290084	II-7	44	HTN, CT	2× NGS	AS-PCR	No PKD Dx, 83 yr	No PKD Dx, 77 yr	6, no PKD Dx	2 no PKD Dx	
M174	II-1	64	Fullness, CT	2× NGS	Sanger	78 yr[a], no PKD Dx	94 yr[a], no PKD Dx	2, no PKD Dx	1 adopted	
290114	II-1	35	Stones, HTN, MR	2× NGS	Sanger	No PKD Dx	No PKD Dx	None	3 no PKD Dx	

AAA, abdominal aortic aneurysm; AS-PCR, allele-specific polymerase chain reaction; BRC, bilateral renal cysts; CNV, copy number variant; CT, computed tomography; Dx, diagnosis; FH, family history; GD, granddaughter; HALT A, relative in the A arm of the HALT-PKD clinical trial; HTN, hypertension; LTFU, lost to follow-up; LR, long-range; MI, myocardial infarction; MLPA, multiplex ligation-dependent probe amplification; MND, mutation not detected; MR, magnetic resonance; MRKH, Mayer Rokitansky, Küster Hauser syndrome; NA, not available; NGS, next-generation sequencing; PC, pancreatic cancer; PH, prenatal hydrocephalous; PKD, polycystic kidney disease; RF, reflux; US, ultrasound; yr, years; +ve, positive; -ve, negative; 2× NGS, both the LR and targeted-capture NGS methods.
[a]Died.

not found by the LR-NGS assay as it spanned the end of a LR-PCR product (Supplementary Table S4), but the deletion was detected by tNGS in 49 of 167 reads (22.7%) from blood-derived DNA, 25.5% in polycystic liver disease tissue (Supplementary Figure S2D). Analysis of breakpoint reads and amplifying across the deletion defined the deletion (Figure 3g; Supplementary Figure S2E). The PKD in II-4 was severe (MIC-1D), resulting in end-stage renal disease at age 55 years, and she also had severe PLD that required partial liver resection (Figure 3h).

M484 II-8 was negative from SS, but a single nucleotide duplication was detected by both LR-NGS, in 1152 of 5207 reads (20.6%), and tNGS, in 518 of 2578 reads (20.1%), and confirmed by re-SS (Figure 3i and j). II-8 had quite severe

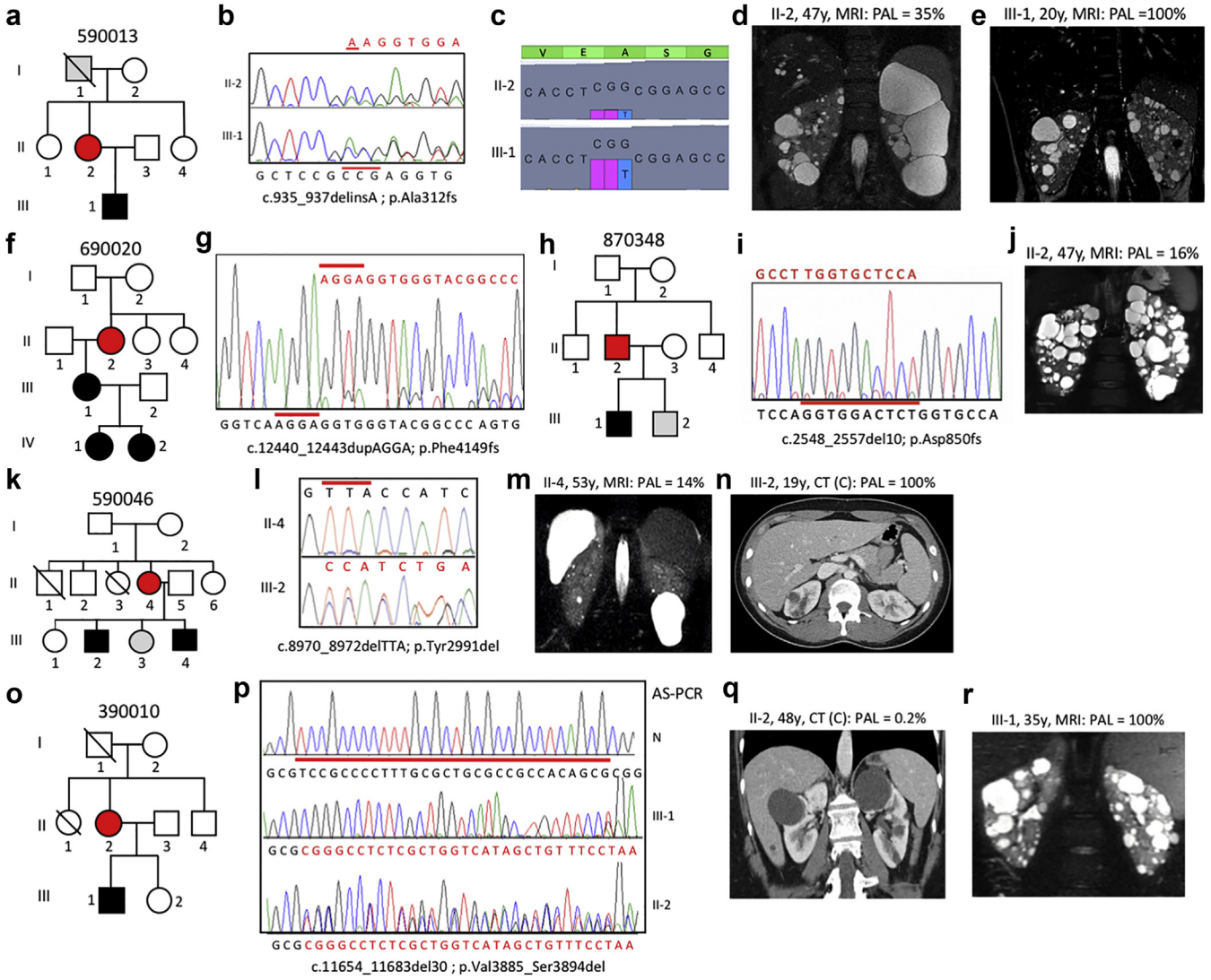

Figure 2 | Pedigree, imaging, and sequencing data of mosaic families segregating the pathogenic variant to the next generation. Pedigree 590013 showing autosomal dominant polycystic kidney disease (ADPKD) in II-2 and III-1, with I-1 found to have a few, likely simple, cysts at age 79 years (**a**). Sanger sequencing (SS) showing the indel (red line) and reduced peak height of the frameshifted sequence (red) in II-2 compared with III-1 (**b**). Targeted-capture next-generation sequencing showing the cytosine–cytosine–guanine (CCG) deletion and adenine (A) insertion (opposite strand shown so the deletion is CGG and the insertion is tyrosine [T]) in a reduced number of reads in II-2 compared with III-1 (**c**). Magnetic resonance imaging (MRI) of II-2 at age 47 years showing asymmetric disease with just a few large cysts in the left kidney (**d**) compared with a more-even distribution in III-1 (**e**). Pedigree 690020 with ADPKD in 3 generations (**f**). SS of II-2 showing the frameshifted sequence following the 4–base pair (bp) duplication at a low level, reflecting mosaicism (**g**). Pedigree of family 870348 with ADPKD in II-2 and III-1 (**h**). SS of II-2 (reverse strand) showing frameshifted sequence due to a 10-bp deletion at a very low level, which is confirmed by allele-specific polymerase chain reaction (AS-PCR; **i**; Supplementary Figure S2B). MRI showing robust PKD in II-2 (**j**). Pedigree 590046 showing the mosaic case (II-4) with 2 affected children (III-2 and III-4; **k**). The inframe codon deletion is seen at only a low level in II-4 compared with III-2 (**l**). MRI of II-4 showing very mild kidney and liver cystic disease (**m**). Contrast (C)-enhanced computed tomography (CT) of III-2 at age 19 years showing a few kidney cysts (**n**). Pedigree 390010 shows ADPKD in the II-2 and III-1 (**o**). SS of the AS-PCR from a normal individual (N), the son (III-1), and the mosaic mother (II-2) shows the 30-bp deletion in the son, but due to the low-level mosaicism, the AS-PCR is not completely specific in II-2, hence the doublet sequence (**p**). CT of II-2 shows just a couple of cysts (**q**), in contrast to the typical PKD shown by MRI in III-1 (**r**). Pedigree: red-shaded, mosaic; gray, equivocal or unknown; white, ADPKD-negative. The percentage of the observed versus expected level of the pathogenic allele (PAL) is indicated next to each radiologic image.

kidney disease (MIC-1C), but normal renal function at age 47 years, and severe PLD requiring cyst aspiration (Figure 3k).

A possible mosaic frameshifting deletion was detected by SS in M375 II-3 that was confirmed and quantified in 930 of 4858 reads (19.1%) by LR-NGS (Figure 3l and m). The ADPKD was mild (MIC-1A), with normal renal function at age 34 years (Figure 3n).

SS showed 290001 II-1 to be negative, but a nonsense pathogenic variant was detected by the LR-NGS, in 1296 of 7347 reads (17.5%), and tNGS, in 1045 of 5061 reads (20.6%), and seen at a low level after re-SS (Figure 3o

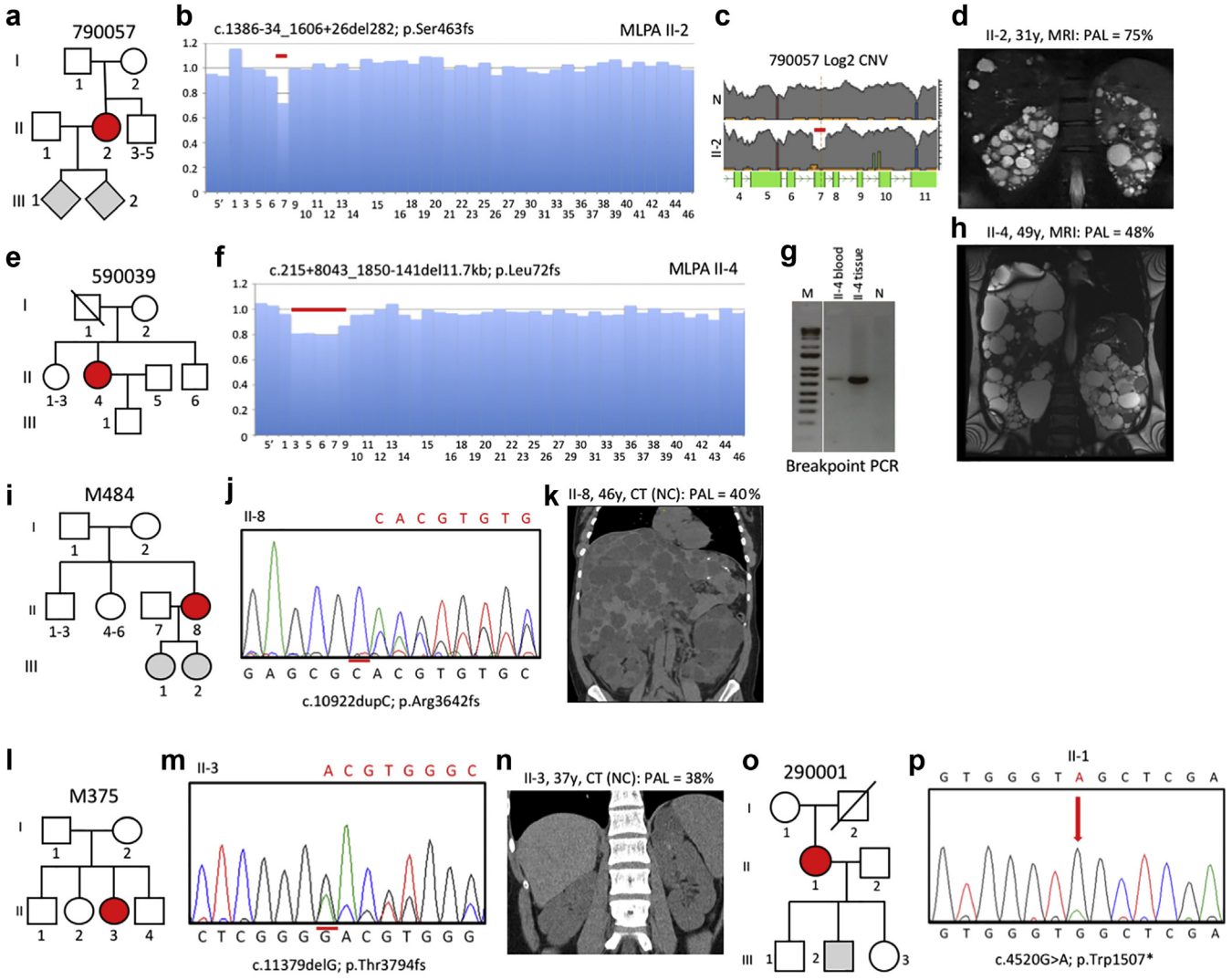

Figure 3 | Pedigree, imaging, and sequencing data of mosaic families not segregating the pathogenic variant (I). Pedigree 790057 showing the mosaic mother (II-2) and her untested offspring (**a**). Screening by multiplex ligation-dependent probe amplification (MLPA) found a possible mosaic deletion of ex7 (**b**) that was confirmed by log2 copy number variant (CNV) analysis of the long-range next-generation sequencing (LR-NGS; **c**). Magnetic resonance imaging (MRI) of II-2 shows typical autosomal dominant polycystic kidney disease (ADPKD) at age 31 years (**d**). Pedigree 590039 shows the mosaic subject (II-4) as the only one affected (**e**). A suspected mosaic *PKD1* deletion was detected by MLPA and confirmed by log2 CNV analysis (**f**; Supplementary Figure S2D). Amplification and Sanger sequencing (SS; Supplementary Figure S2E) of a specific breakpoint fragment defined the deletion in blood and liver tissue–derived DNA (**g**). MRI of II-4 shows significant kidney disease at age 49 years (prior to end-stage renal disease) and severe polycystic liver disease (PLD; after partial liver resection; **h**). Pedigree M484 showing 2 untested daughters of the mosaic case (II-8; **i**). SS confirmation of the mosaic single nucleotide duplication in II-8 (**j**). Non-contrast (NC) enhanced computed tomography (CT) of II-8 at age 46 years shows significant PKD and severe PLD (**k**). Pedigree M375 shows just one affected subject (II-3; **l**). SS shows II-3 is mosaic for a single nucleotide deletion (**m**). CT of II-3 at age 37 years shows very mild kidney disease (**n**). Pedigree 290001 shows the mosaic subject (II-1) and 3 children without PKD or untested (**o**). SS of II-1 confirms mosaicism of a nonsense change (**p**). Pedigree: red-shaded, mosaic; gray, equivocal or unknown; white, ADPKD-negative. The percentage of the observed versus expected level of the pathogenic allele (PAL) is indicated next to each radiologic image. A, adenine; C, cytosine; G, guanine; PCR, polymerase chain reaction; T, thymine.

and p). Ultrasound identified multiple bilateral cysts, and the patient had Stage 3b CKD at age 66 years.

Initial SS of 870005 II-2 was negative, but tNGS identified a frameshifting pathogenic variant in 84 of 566 reads (14.8%), which was subsequently seen at a low level in the SS by visual inspection (Figure 4a and b). This patient had moderately severe PKD (MIC-1C), and moderate PLD, but normal renal function at age 54 years (Figure 4c).

SS was negative in M646 II-3, but tNGS identified the missense variant p.Pro2809Leu in 454 of 3392 reads (13.4%), which was subsequently seen at a low level by SS (Figure 4d and e). p.Pro2809Leu is a non-conservative substitution of a residue invariant in orthologs to fish, is not listed in gnomAD,[24] and has been described as a likely pathogenic variant (Supplementary Table S3).[14] II-3 had relatively small, asymmetric kidneys (MIC-1B; Figure 4f) and had Stage 3b CKD at age 60 years.

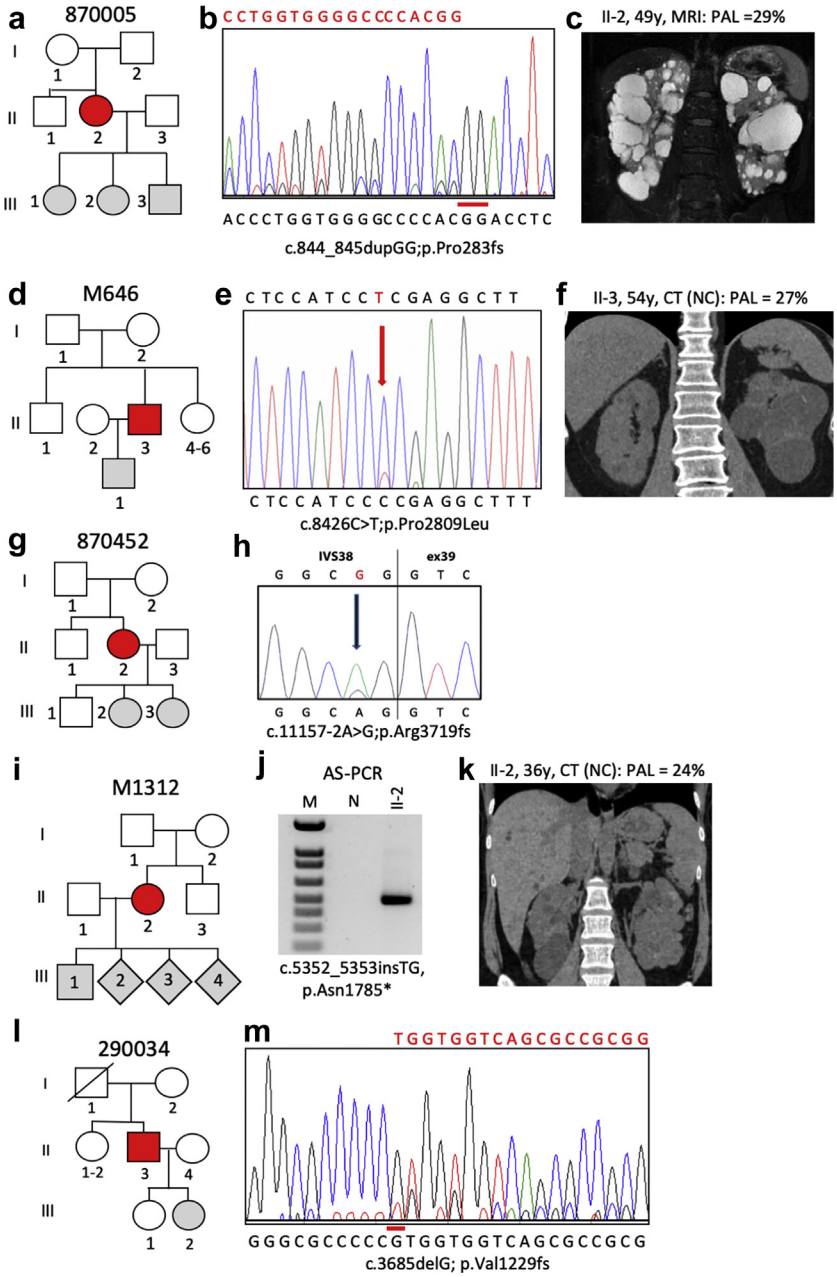

Figure 4 | Pedigree, imaging, and sequencing data of mosaic families not segregating the pathogenic variant (II). Pedigree 870005; the mosaic subject (II-2) has 3 untested children (**a**). Sanger sequencing (SS) confirmation in II-2 of mosaicism of the guanine–guanine (GG) duplication (reverse strand shown; **b**). Magnetic resonance imaging (MRI) of II-2 at age 49 years shows multiple large cysts (**c**). Pedigree M646; the mosaic proband (II-3) has an untested son (**d**). SS confirms mosaicism for a previously described missense substitution in II-3 (**e**). Computed tomography (CT) imaging of II-3 at age 54 years shows bilateral disease with large cysts in the left kidney (**f**). Pedigree 870452 showing 3 offspring of the mosaic case II-2 (**g**). SS of II-2 confirms mosaicism for a typical splicing variant (**h**). Pedigree M1312 shows mosaicism in II-2 with 4 untested children (**i**). Allele-specific polymerase chain reaction (AS-PCR) shows a specific fragment just in II-2 but not the normal (N) control, which was confirmed to have the thymine (T)G insertion, by SS of the product (**j**; Supplementary Figure S2F). CT of II-2 at age 36 years shows bilateral cysts with several large cysts in the right kidney (**k**). Pedigree 290034 indicates mosaicism in II-3 and 2 children either negative or untested (**l**). SS of II-3 confirms mosaicism of a G deletion (**m**). Pedigree: red-shaded, mosaic; gray, equivocal or unknown; white, ADPKD-negative. The percentage of the observed versus expected level of the pathogenic allele (PAL) is indicated next to each radiologic image. A, adenine; C, cytosine.

870452 II-1 was screened only by tNGS, which detected a typical splicing change in 162 of 1208 reads (13.4%), which was confirmed by SS (Figure 4g and h). The patient had normal renal function at age 57 years.

M1312 II-2 was screened initially by tNGS, which revealed a frameshifting insertion in 199 of 1637 reads (12.2%). This insertion was not detected by SS, but AS-PCR amplified from the patient's DNA and SS of the AS-PCR

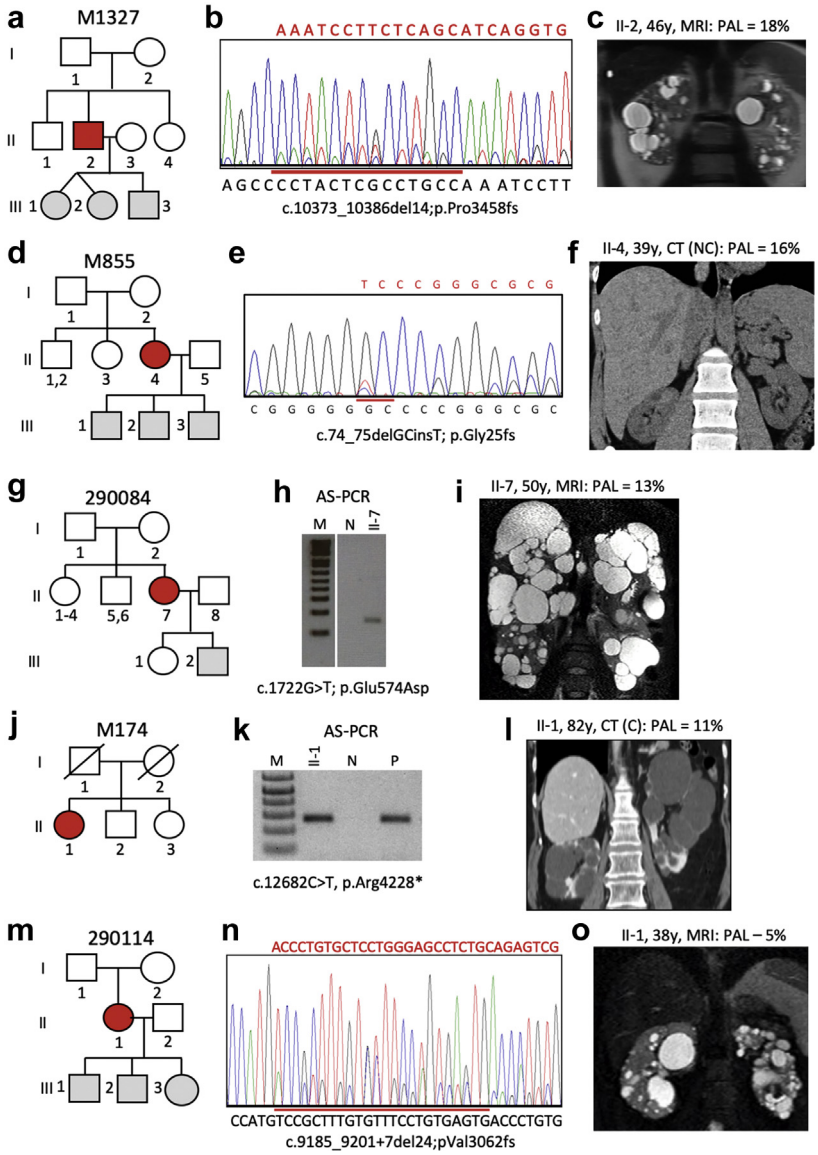

Figure 5 | Pedigree, imaging, and sequencing data of mosaic families not segregating the pathogenic variant (III). Pedigree M1327 shows the mosaic proband (II-2) has untested twin girls and a son (**a**). Sanger sequencing (SS) of II-2 confirms mosaicism for a 14-bp deletion (**b**). Just a few bilateral cysts are detected in II-2 by magnetic resonance imaging (MRI) at age 46 years (**c**). The mosaic proband in M855 (II-4) has 3 untested children (**d**). SS of II-4 confirms mosaicism of a deletion/insertion (**e**). Computed tomography (CT) of II-4 at age 39 years shows just a few small cysts in the kidney and liver (**f**). Pedigree 290084 shows 2 offspring of the mosaic subject (II-7) either negative for polycystic kidney disease (PKD) or untested (**g**). Allele-specific polymerase chain reaction (AS-PCR) shows the mutant allele just in II-7 but not a control (N), and sequencing confirms the substitution (**h**; Supplementary Figure S2G). MRI of II-7 shows moderate kidney disease and severe polycystic liver disease (**i**). The mosaic proband (II-1) in M174 is the only affected member (**j**). AS-PCR shows that II-1 has p.Arg4228*, which is also found in a positive control (P) but not an individual without this change (N), and SS shows the substitution at a very low level (**k**; Supplementary Figure S2H). CT of II-1 at age 82 years, shortly before end-stage renal disease, shows a few large cysts in both kidneys (**l**). Pedigree 290114 shows the mosaic individual (II-1) has 3 untested children (**m**). SS of II-1 shows mosaicism for a 24–base pair splice site spanning deletion (**n**). II-1 has mild cystic disease with a few moderately sized cysts (**o**). Pedigree: red-shaded, mosaic; gray, equivocal or unknown; white, autosomal dominant polycystic kidney disease–negative. The percentage of the observed versus expected level of the pathogenic allele (PAL) is indicated next to each radiologic image. A, adenine; C, cytosine; G, guanine; T, thymine.

product confirmed the insertion (Figure 4i and j; Supplementary Figure S2F). Imaging showed multiple kidney cysts, including a large one, but renal function was normal at age 36 years (Figure 4k).

SS of 290034 II-3 was negative, but analysis by both LR-NGS, in 786 of 6407 reads (12.3%), and tNGS, in 523 of 4352 reads (12.0%), detected a mosaic frameshifting deletion that was subsequently confirmed by close examination of the SS (Figure 4l and m). II-3 had moderate kidney disease (MIC-1C and Stage 3b CKD at age 68 years).

In patient M1327 II-2, no mutation was detected by clinical SS, but tNGS detected a frameshifting deletion in 134 of 1489 reads (9.0%), which was confirmed by repeat SS; the parents were negative for the pathogenic variant (Figure 5a

and b). II-2 had relatively mild PKD, MIC-1B, and normal renal function at age 48 years (Figure 5c).

A pathogenic variant was suspected but undefined by SS in M855 II-4 and was then characterized by LR-NGS as an indel in 725 of 8889 reads (8.2%; Figure 5d and e). The kidney phenotype was mild cystic disease (MIC-1B) with normal renal function at age 47 years (Figure 5f).

No mutation was detected in 290084 II-7 by initial SS, but a conservative missense change (p.Glu574Asp) was found by both LR-NGS, in 423 of 7044 reads (6.0%), and tNGS, in 279 of 3540 reads (7.3%), and confirmed by AS-PCR (Figure 5g and h; Supplementary Figure S2G). The substitution, c.1722G>T, changes the last nucleotide of exon 8 and is predicted to result in loss of the IVS8 donor site (Supplementary Figure S2G legend; Supplementary Table S3). The patient has normal renal function at age 53 years but relatively large kidneys (MIC-1C) and severe PLD (Figure 5i).

Initial SS of M174 II-1 was negative, but a nonsense variant was detected by LR-NGS, in 427 of 6018 reads (7.1%), and tNGS, in 40 of 1159 reads (3.5%), and confirmed by AS-PCR and SS (Figure 5j and k; Supplementary Figure S2H). The patient had rather few, larger cysts in each kidney and reached end-stage renal disease at age 83 years (Figure 5l).

290114 II-1 was NMI from initial SS, but the LR-NGS, in 304 of 7506 reads (4.1%), and tNGS, in 46 of 3490 reads (1.3%), identified a deletion extending over a splice junction. This was subsequently confirmed by re-SS (Figure 5m and n). This patient had relatively mild cystic disease (MIC-1B) and normal renal function at age 40 years (Figure 5o).

Phenotypic features of the mosaic individuals

We compared the estimated glomerular filtration rate and height-adjusted total kidney volume for the mosaic cases to a nonmosaic Mayo PKD1 population with similar mutation types—truncating or strongly predicted nontruncating mutations (mutation strength groups 1 and 2).[9] This analysis showed that the mosaic group had a greater estimated glomerular filtration rate of 30.2 ml/min per 1.73 m^2 ($P < 0.001$) and a height-adjusted total kidney volume 32.5% ($P = 0.021$) smaller than that of the controls, but there was little correlation between the level of the mosaic mutant allele and either phenotype (Figure 6a and b).

DISCUSSION

We describe here 2 NGS methods to robustly detect mosaic pathogenic variants (~4%–50% expected allele level) in the *PKD1* or *PKD2* gene, including in the duplicated region of *PKD1*. Unlike in previous descriptions of ADPKD mosaicism, 15 pathogenic variants were detected when just one family member was affected. When both methods were employed (6 cases), there was good agreement in the mutant allele level, which was more quantifiable and reliable than that from SS. Both methods have good read depth over most parts of the screened genes, although read depth was lower for both in

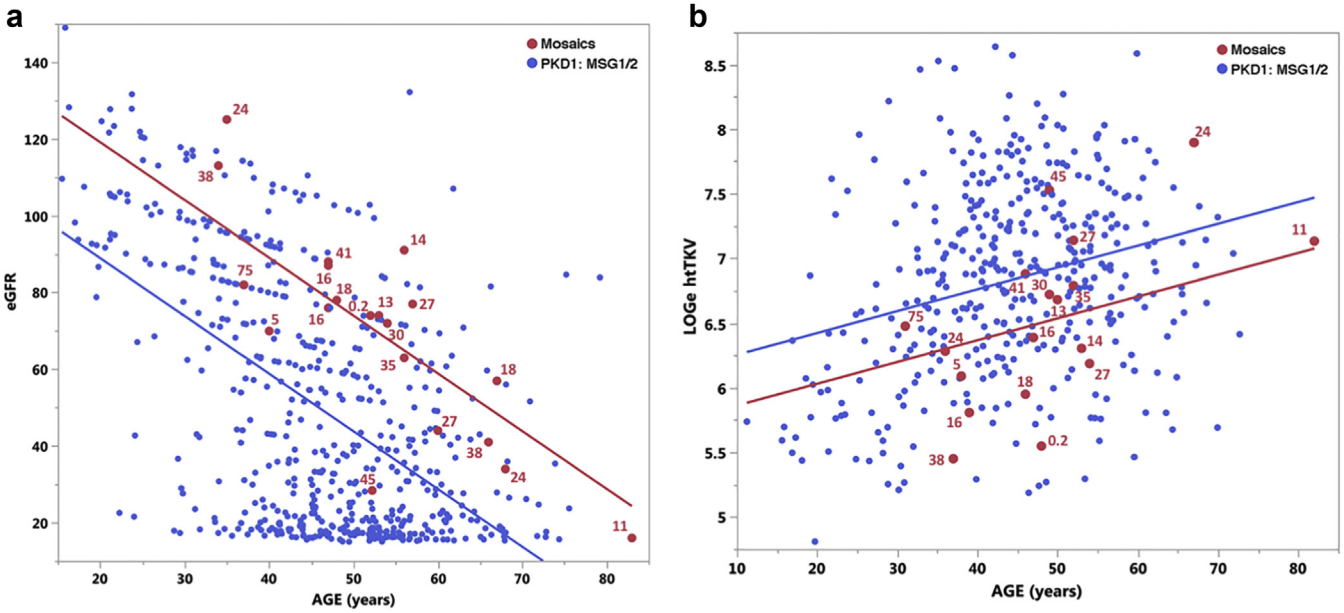

Figure 6 | Regression comparison of estimated glomerular filtration rate (eGFR) and height-adjusted total kidney volume (htTKV) in mosaic subjects compared to PKD1 controls. The control populations (blue) are PKD1 patients with truncating (mutation strength group [MSG]1) or strongly predicted nontruncating changes (MSG2)[9] from a Mayo Clinic Translational PKD Center cohort without known mosaicism; n = 550 for eGFR and 403 for htTKV. The mosaic population is indicated in red, and the percentage level of the mosaic allele compared to a fully penetrant allele is listed for each case. The renal function analysis shows that the mosaic population (red) has a significantly higher eGFR than the controls (blue; **a**). Analysis of renal structure shows that the mosaic population has a significantly lower htTKV than the controls. The htTKV is plotted on a log2 scale (LOGe) (**b**). No correlation was observed between the level of mosaicism and disease severity (eGFR or htTKV).

very guanine–cytosine–rich regions (Supplementary Table S2). However, the much easier application of tNGS versus LR-PCR means it is likely to be more widely employed.[15,17,18] The greater read depth, plus better coverage of *PKD1,* shows the value of a targeted approach for screening (especially for mosaicism) of this gene compared to whole-exome sequencing.[17,18,25] Here, we did not attempt to identify patients with possible high-level mosaicism (50%–90% expected allele level), as further study is needed to reliably differentiate mosaicism from *de novo* germline mutations.

Detecting mosaicism is important, as it can genetically resolve SS NMI cases (13 families in this study). Also, it provides important prognostic information; on average, the kidney disease in mosaics is milder than expected for the mutation type, with important implications for the expected renal disease severity in offspring compared with the parent. However, the precise level of mosaicism in blood cell DNA did not strongly correlate with disease severity, presumably reflecting the fact that the level of the mutant allele in the kidney can diverge considerably from that in blood cells. Interestingly, 3 mosaics had severe PLD, consistent with previous data showing that the ADPKD genotype is less important for the development of liver versus kidney disease.[26] In the one case for which severe PLD tissue was assayed, the level of the mutant allele was only slightly higher than that in the blood cell DNA.

In transmitted cases, knowledge that the disease is likely to be more severe in offspring is important. In the families studied here, the mutant allele was transmitted in 25% of cases. There is likely a positive bias in detecting cases with a fully penetrant offspring, but many families had only unscreened or young offspring, or no offspring, and so the transmission rate may be underestimated. Nevertheless, it seems likely that >50% of mosaic cases are sporadic and are not transmitted. In males, fuller analysis of germ cells will determine the level of mixed rather than strictly somatic mosaics and the level of germline mosaicism. Overall, 16 of 20 mosaic individuals were female, suggesting an enrichment, but the difference between this level and that in the female enriched control population was not statistically significant ($P = 0.11$).

Mosaicism is often considered an explanation for unilateral and severely asymmetric cases that usually have a negative family history. Indeed, we did identify 6 cases with asymmetric or lopsided disease. However, over the whole cohort, this was not a consistent feature, and 26 fully unilateral or markedly asymmetric cases remained unresolved after these NGS-based screens. This lack of resolution is likely due to the fact that the mosaics identified by screening blood cell DNA have broad penetrance of the mutant allele in the body's organs. Screening DNA isolated from other tissues, such as cells isolated from urine, buccal cells, hair roots, skin fibroblasts, and sperm, plus methods to detect pathogenic variants at <2%, may solve these cases. Although not a significant problem in our study, the degree to which the duplicated *PKD1* gene will complicate detection of very low-level mosaicism remains to be determined.

All of the detected mosaic cases were PKD1. An enrichment for PKD1 would be expected as it is the most common ADPKD gene (~78% of cases) and a larger mutational target (~13-kb coding region compared with ~3 kb for *PKD2*), and mosaic PKD2 subjects may have a very mild phenotype and so not be recognized as having PKD. But it does raise the question again of whether *PKD1* is unusually prone to *de novo* mutations.[27] Most mutations (15 of 20) were deletions or insertions (~39% of germline *PKD1* mutations), 14 of which were frameshifting, including 6 deletions or insertions >10 bp, and two >250 bp. It has been previously described that mosaicism of larger rearrangements is more common than it is for base-pair changes,[28] but whether the predominance of indels here is just due to ease of detection is unclear.

The HALT PKD cohort is a typical ADPKD population in which patients were hypertensive at baseline, and recruited patients had either normal renal function (ages 15–49 years; study A) or an estimated glomerular filtration rate of 25–60 ml/min per 1.73 m^2 (ages 18–64 years; study B). Notably, there was no kidney size requirement for recruitment, and the finding of 5 different genes in this population shows its diversity.[9,11,12,29] All HALT PKD patients with DNA available were screened by SS,[9] and unresolved and suspected mosaic cases were rescreened by NGS (LR and/or tNGS). Overall, 10 of 831 HALT PKD families (1.2%) were shown to have ADPKD originating from a mosaic case (Figure 1). A similar level (0.9%) was found from the newly screened patients, employing tNGS.

In the LR-NGS cohort, in which all patients had a negative or equivocal family history and NMI from SS, 7 cases were newly resolved as mosaic (Figure 1). Removing the patients resolved in other ways (fully penetrant *PKD1*/PKD2 pathogenic variants or other disease genes), the mosaics were equivalent to 8.9% of the residual families (Figure 1). Therefore, in a typical ADPKD population, ~1% of families, and ~10% of NMI families, without a clear family history, are readily resolvable mosaics. With inclusion of very low-level (<4% expected level) and high-level (>50%) mosaics, and analysis of other DNA sources, the total number of mosaics would likely be even higher, although the representation of mosaics in a population selected for rapidly progressive disease would likely be lower.[30,31]

METHODS

Study participants and clinical analysis

The participants were recruited through various ADPKD cohorts: the HALT-PKD clinical trial (n = 10 positive cases: 590013, 690020, 590046, 390010, 790057, 590039, 290001, 290034, 290084, 290114)[9,32,33]; the ADPKD Modifier Study (n = 3: 870348, 870005, 870452); and patients at the Mayo Clinic Translational PKD Center (n = 7: M484, M375, M646, M1312, M1327, M855, M174; Figure 1). The relevant institutional review boards or ethics committees approved all studies, and participants gave informed consent. Clinical and imaging data were obtained by review of clinical and study records. Kidney function was calculated from clinical serum creatinine measurements with the Chronic Kidney Disease Epidemiology Collaboration (CKD-EPI) formula.[34] Blood samples for

standard DNA isolation were collected from the probands and all available family members.

NGS of *PKD1/PKD2* LR-PCR amplicons (LR-NGS)

A total of 110 ADPKD patients were screened that had a negative/equivocal family history and were *PKD1/PKD2* NMI by SS (Figure 1). Four of the selected patients were suspected mosaic cases based on either prior SS or family data. The samples were analyzed employing a modification of the LR-PCR and NGS approach,[15] which is described in detail in the Supplementary Methods and Supplementary Table S4. For the bioinformatics analysis, FASTQ files were aligned to the hg19 reference genome using bwa-mem (VN:V7.10) with default options. Variant calling was performed using the GATK (VN:3.6) Haplotype Caller. Generated vcf files were prioritized for variants fulfilling the following criteria: genotype quality ≥20; read depth ≥20; alternate allele frequency ≥3%; forward/reverse read balance ≥0.25; ExAc/ESP6500/1000 genome allele frequency ≤0.1%; frequency count within screened patient population <4; exonic +/-15 bp; nonsynonymous, dbNSFP evaluation ≥2 as damaging (Lrt, MetaLr, PolyPhen2, Provean, SIFT). BAM files of variants of interest were reviewed and designated as possible mosaics if the alternate allele was present in 2%–35% of reads.

Targeted next-generation sequencing (tNGS)

Samples were run on a custom Agilent SureSelect gene panel containing the coding regions ±50 bp of either 65[12] or 137 genes (Supplementary Table S1). Library preparation, sequencing, and sequence alignment was performed as described.[12] The SNP and Variation Suite (SVS, Golden Helix) was used for small nucleotide variant mining, utilizing the following filtering thresholds: variant locus read-depth (DP) ≥10 and quality (GQ) ≥20; GnomAD, minor allele frequency (MAF) ≤1.0%; and removal of noncoding variants >15 bp from the splice site. The remaining variants were individually evaluated for pathogenicity based on inclusion in the online ADPKD database (pkdb.pkdcure.org); or predicted loss of function, or Sorting Intolerant From Tolerant (SIFT; https://sift.bii.a-star.edu.sg/) score ≤0.10 and alignGVGD class ≥C35, and not present in an orthologous sequence; or predicted to alter splicing by Berkeley Drosophila Genome Project (BDGP) and Human Splicing Finder 3.0. BAM files of variants of interest were reviewed and designated as possible mosaics if the alternate allele was present in 1%–35% of reads. Large copy number variants were assessed by calculating the LOG2 ratio of actual read-depth over the expected read-depth for a given locus. Variants with LOG2 ratios between 0.5 and 0.1 or –0.2 and –0.9 were considered mosaic candidates. BAM files were reviewed to identify exact breakpoints of the copy number variants, and the final level of mosaicism was calculated based on the change of read-depth at the 5' end of the rearrangement.

Confirmation of variants by SS, MLPA, or AS-PCR

All changes were confirmed by SS for *PKD1* as previously described.[14] When family samples were available, segregation analysis of the variant of interest was performed. MLPA was performed employing the MRC-Holland (Amsterdam, The Netherlands) kits. For AS-PCR, allele-specific primers were designed for mosaic variants which were either not detected or poorly detected by SS. Either the forward or reverse primer was designed specifically to match the pathogenic variant (Supplmentary Table S5), with a second mismatch often introduced,[35] and used to PCR amplify the mosaic variant using standard methods.

Analysis of phenotypic endpoints of the mosaic population

The most recent estimated glomerular filtration rate and height-adjusted total kidney volume available on mosaic cases and PKD1 controls (MSG 1 and 2) were employed for the regression analysis to correlate the age and phenotypic endpoints.

DISCLOSURE

All the authors declared no competing interests.

ACKNOWLEDGMENTS

We thank the families and coordinators for involvement in the study and Andrew Metzger and Timothy Kline (Mayo Clinic). The study was supported by: National Institute of Diabetes and Digestive and Kidney Diseases (NIDDK) grant DK058816 (to PCH); the Mayo Clinic Robert M. and Billie Kelley Pirnie Translational Polycystic Kidney Disease Center (DK090728; to VET); an American Society of Nephrology (ASN) Foundation Ben J Lipps Fellowship (to KH); an ASN Kidney Research Fellowship (to EC-LG); the Fulbright Association and the Foundation Monaham (EC-LG); the Zell Family Foundation, and Robert M. and Billie Kelley Pirnie. The HALT-PKD studies were supported by NIDDK cooperative agreements (DK062410, DK062408, DK062402, DK082230, DK062411, and DK062401) and National Center for Research Resources General Clinical Research Centers (RR000039, RR000585, RR000054, RR000051, RR023940, RR001032) and National Center for Advancing Translational Sciences Clinical and Translational Science Awards (RR025008, TR000454, RR024150, TR00135, RR025752, TR001064, RR025780, TR001082, RR025758, TR001102, RR033179, TR000001). The ADPKD Modifier Study is supported by NIDDK grant DK079856.

We thank the other HALT PKD and/or ADPKD Modifier Investigators as well: A. Yu, F.T. Winklhofer (Kansas University Medical Center, Kansas City, KS), K.Z. Abebe, C.G. Patterson (University of Pittsburgh, Pittsburgh, PA), R.W. Schrier, G.M. Brosnahan (University of Colorado Denver, Aurora, CO), D.C. Miskulin (Tufts University, Boston, MA), W.E. Braun (Cleveland Clinic, Cleveland, OH), P.G. Czarnecki (Brigham and Women's Hospital, Boston, MA), F.T. Chebib, M.C. Hogan (Mayo Clinic, Rochester, MN), M. Mrug (University of Alabama at Birmingham, Birmingham, AL), Y. Pei, (University of Toronto, Toronto, Ontario, Canada), R. Sandford (University of Cambridge, Cambridge, UK), H. Rennert (The Rogosin Institute, New York, NY), Y. Le Meur (Université de Brest, Brest, France), T. Watnick (University of Maryland, Baltimore, MD), D.J.M. Peter (Leiden University Medical Center, Leiden, The Netherlands), R.T. Gansevoort (University Medical Center Groningen, Groningen, The Netherlands), N. Demoulin (Université Catholique de Louvain, Louvain, Belguim), and O. Devuyst (University Hospital of Zürich, Zurich, Switzerland).

SUPPLEMENTARY MATERIAL

Supplementary File (PDF)

Supplementary Methods. LR-NGS methods.
Figure S1. Analysis of 2 false-positive "mosaic" PKD1 families.
Figure S2. Details of mosaic positive PKD1 families.
Table S1. Genes included on the 137-gene panel.
Table S2. Mean read counts for the exonic regions of *PKD1* and *PKD2* by the 65- and 137-gene panel.
Table S3. Details of the *PKD1* pathogenic variants detected in the 20 mosaic families.
Table S4. Details of primers used for amplification of *PKD1* and *PKD2* for the LR-NGS protocol.
Table S5. Primers and conditions for AS-PCR.

REFERENCES

1. Sampson JR, Scahill SJ, Stephenson JB, et al. Genetic aspects of tuberous sclerosis in the west of Scotland. *J Med Genet*. 1989;26:28–31.

2. Tyburczy ME, Dies KA, Glass J, et al. Mosaic and intronic mutations in TSC1/TSC2 explain the majority of TSC patients with no mutation identified by conventional testing. *PLoS Genet*. 2015;11:e1005637.
3. Rossetti S, Strmecki L, Gamble V, et al. Mutation analysis of the entire PKD1 gene: genetic and diagnostic implications. *Am J Hum Genet*. 2001;68:46–63.
4. Iliuta IA, Kalatharan V, Wang K, et al. Polycystic kidney disease without an apparent family history. *J Am Soc Nephrol*. 2017;28:2768–2776.
5. Torres VE, Harris PC, Pirson Y. Autosomal dominant polycystic kidney disease. *Lancet*. 2007;369:1287–1301.
6. Gabow PA, Johnson AM, Kaehny WD, et al. Factors affecting the progression of renal disease in autosomal-dominant polycystic kidney disease. *Kidney Int*. 1992;41:1311–1319.
7. Cornec-Le Gall E, Audrezet MP, Chen JM, et al. Type of PKD1 mutation influences renal outcome in ADPKD. *J Am Soc Nephrol*. 2013;24:1006–1013.
8. Irazabal MV, Rangel LJ, Bergstralh EJ, et al. Imaging classification of autosomal dominant polycystic kidney disease: a simple model for selecting patients for clinical trials. *J Am Soc Nephrol*. 2015;26:160–172.
9. Heyer CM, Sundsbak JL, Abebe KZ, et al. Predicted mutation strength of nontruncating PKD1 mutations aids genotype-phenotype correlations in autosomal dominant polycystic kidney disease. *J Am Soc Nephrol*. 2016;27:2872–2884.
10. Clissold RL, Hamilton AJ, Hattersley AT, et al. HNF1B-associated renal and extra-renal disease—an expanding clinical spectrum. *Nat Rev Nephrol*. 2015;11:102–112.
11. Porath B, Gainullin VG, Cornec-Le Gall E, et al. Mutations in GANAB, encoding the glucosidase ii alpha subunit, cause autosomal-dominant polycystic kidney and liver disease. *Am J Hum Genet*. 2016;98:1193–1207.
12. Cornec-Le Gall E, Olson RJ, Besse W, et al. Monoallelic mutations to DNAJB11 cause atypical autosomal-dominant polycystic kidney disease. *Am J Hum Genet*. 2018;102:832–844.
13. Cornec-Le Gall E, Torres VE, Harris PC. Genetic complexity of autosomal dominant polycystic kidney and liver diseases. *J Am Soc Nephrol*. 2018;29:13–23.
14. Rossetti S, Consugar MB, Chapman AB, et al. Comprehensive molecular diagnostics in autosomal dominant polycystic kidney disease. *J Am Soc Nephrol*. 2007;18:2143–2160.
15. Rossetti S, Hopp K, Sikkink RA, et al. Identification of gene mutations in autosomal dominant polycystic kidney disease through targeted resequencing. *J Am Soc Nephrol*. 2012;23:915–933.
16. Tan AY, Michaeel A, Liu G, et al. Molecular diagnosis of autosomal dominant polycystic kidney disease using next-generation sequencing. *J Mol Diagn*. 2014;16:216–228.
17. Trujillano D, Bullich G, Ossowski S, et al. Diagnosis of autosomal dominant polycystic kidney disease using efficient PKD1 and PKD2 targeted next-generation sequencing. *Mol Genet Genomic Med*. 2014;2:412–421.
18. Eisenberger T, Decker C, Hiersche M, et al. An efficient and comprehensive strategy for genetic diagnostics of polycystic kidney disease. *PLoS One*. 2015;10:e0116680.
19. Braun WE, Abebe KZ, Brosnahan G, et al. ADPKD progression in patients with no apparent family history and no mutation detected by Sanger sequencing. *Am J Kidney Dis*. 2018;71:294–296.
20. Connor A, Lunt PW, Dolling C, et al. Mosaicism in autosomal dominant polycystic kidney disease revealed by genetic testing to enable living related renal transplantation. *Am J Transplant*. 2008;8:232–237.
21. Consugar MB, Wong WC, Lundquist PA, et al. Characterization of large rearrangements in autosomal dominant polycystic kidney disease and the *PKD1/TSC2* contiguous gene syndrome. *Kidney Int*. 2008;74:1468–1479.
22. Reiterova J, Stekrova J, Merta M, et al. Autosomal dominant polycystic kidney disease in a family with mosaicism and hypomorphic allele. *BMC Nephrol*. 2013;14:59.
23. Tan AY, Blumenfeld J, Michaeel A, et al. Autosomal dominant polycystic kidney disease caused by somatic and germline mosaicism. *Clin Genet*. 2015;87:373–377.
24. Karczewski KJ, Francioli LC, Tiao G, et al. Variation across 141,456 human exomes and genomes reveals the spectrum of loss-of-function intolerance across human protein-coding genes [e-pub ahead of print]. *BioRxiv*. https://doi.org/10.1101/531210. Accessed October 31, 2019.
25. Tan AY, Zhang T, Michaeel A, et al. Somatic mutations in renal cyst epithelium in autosomal dominant polycystic kidney disease. *J Am Soc Nephrol*. 2018;29:2139–2156.
26. Chebib FT, Jung Y, Heyer CM, et al. Effect of genotype on the severity and volume progression of polycystic liver disease in autosomal dominant polycystic kidney disease. *Nephrol Dial Transplant*. 2016;31:952–960.
27. Liu G, Myers S, Chen X, et al. Replication fork stalling and checkpoint activation by a PKD1 locus mirror repeat polypurine-polypyrimidine (Pu-Py) tract. *J Biol Chem*. 2012;287:33412–33423.
28. Kozlowski P, Roberts P, Dabora S, et al. Identification of 54 large deletions/duplications in TSC1 and TSC2 using MLPA, and genotype-phenotype correlations. *Hum Genet*. 2007;121:389–400.
29. Cornec-Le Gall E, Chebib FT, Madsen CD, et al. The value of genetic testing in polycystic kidney diseases illustrated by a family with PKD2 and COL4A1 mutations. *Am J Kidney Dis*. 2018;72:302–308.
30. Torres VE, Chapman AB, Devuyst O, et al. Tolvaptan in patients with autosomal dominant polycystic kidney disease. *N Engl J Med*. 2012;367:2407–2418.
31. Cornec-Le Gall E, Blais J, Irazabal MV, et al. Can we further enrich ADPKD clinical trials for rapidly progressive patients? Application of the PROPKD score in the TEMPO trial. *Nephrol Dial Transpl*. 2018;33:645–652.
32. Schrier RW, Abebe KZ, Perrone RD, et al. Blood pressure in early autosomal dominant polycystic kidney disease. *N Engl J Med*. 2014;371:2255–2266.
33. Torres VE, Abebe KZ, Chapman AB, et al. Angiotensin blockade in late autosomal dominant polycystic kidney disease. *N Engl J Med*. 2014;371:2267–2276.
34. Levey AS, Stevens LA, Schmid CH, et al. A new equation to estimate glomerular filtration rate. *Ann Intern Med*. 2009;150:604–612.
35. Newton CR, Graham A, Heptinstall LE, et al. Analysis of any point mutation in DNA. The amplification refractory mutation system (ARMS). *Nucl Acids Res*. 1989;17:2503–2516.